Electronic Supplementary Material (ESI) for Journal of Materials Chemistry A.

Organic-inorganic hybrid photocatalyst consisting of highly conjugated metal complex and graphitic carbon nitride for efficient hydrogen evolution and Cr(VI) reduction.

Bishal Das[a#], Laxmi Prasad Rao Pala[b#], Manoj Kumar Mohanta[c], Meghali Devi[a], Debarati Chakraborty[a], Nageswara Rao Peela[b], Mohammad Qureshi[c], Siddhartha Sankar Dhar[a*],

[a] Department of Chemistry, National Institute of Technology, Silchar, Silchar, Cachar, 788010, Assam, India. E-mail: ssd@che.nits.ac.in

[b] Department of Chemical Engineering, Indian Institute of Technology, Guwahati

[c] Department of Chemistry, Indian Institute of Technology, Guwahati

[#] Equal contribution

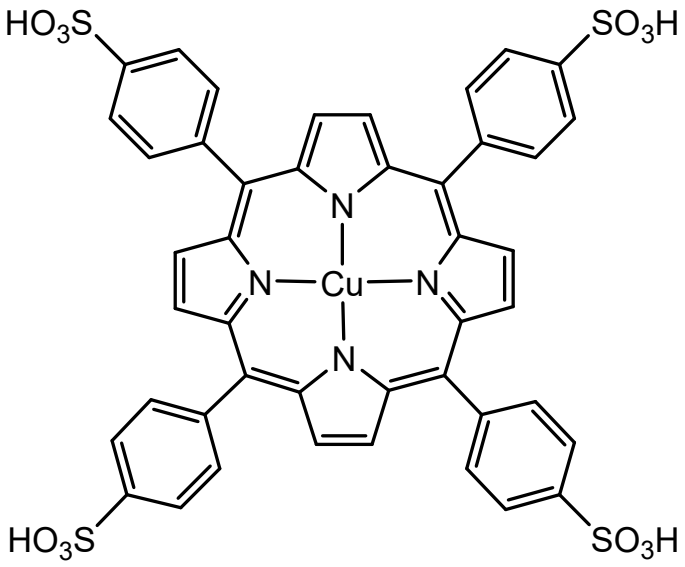

Figure S1. Schematic structure of Cu-Por

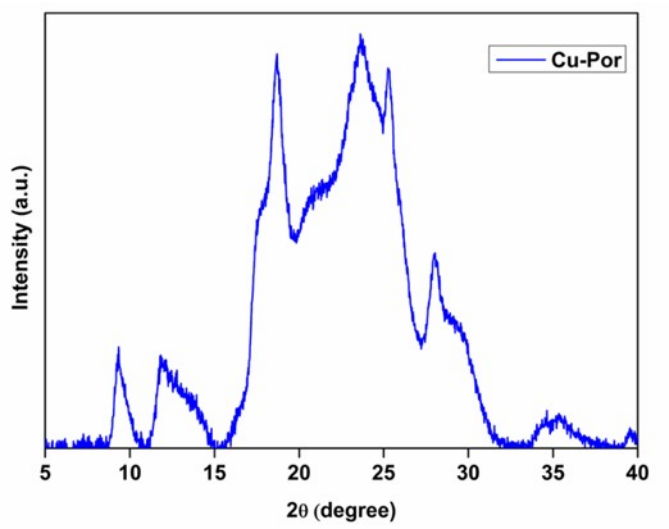

Figure S2. XRD of Cu-Por

The XRD data of Cu-Por shows peaks at 9.3°, 11.8°, 18.7°, 23.5°, 25.1° and 28.1° which are consistent with the literature.[S1,S2]

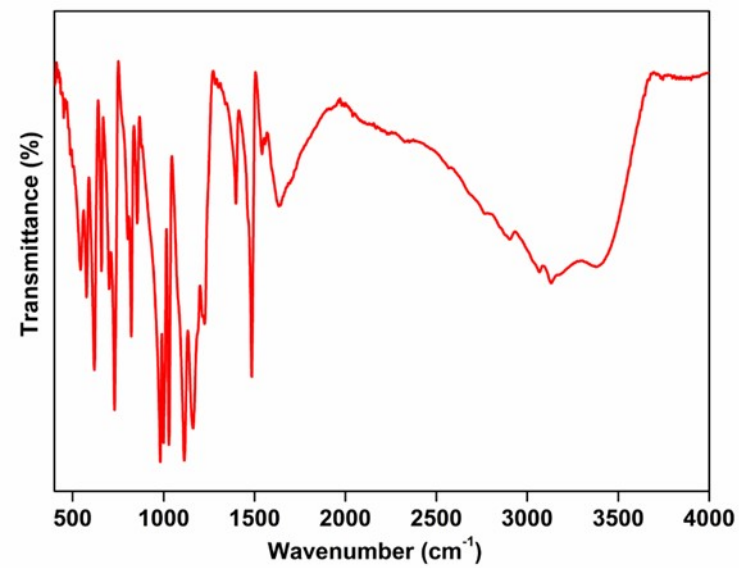

Figure S3. FT-IR spectra of Cu-Por

The peaks at 570 and 1020 cm^{-1} are assigned to S-O and O=S=O bonds respectively. The peaks at 729, 1502, 1636 cm^{-1} can be allocated to the benzene ring. The peaks at 550, 850, 1064, 1120 and 1410 cm^{-1} due to in-plane modes of pyrrole rings. The peak at 1166 cm^{-1} is due to N-Cu vibration. The peaks at 1542 and 1643 cm^{-1} are assigned to C=N vibrations. Other peaks in the range of 500-800 cm^{-1} are due to bending vibrations of C-H and C-C. The peak in the range of 3000-3600 cm^{-1} are due to =C-H stretching and absorbed water molecules.[S3,S4]

Wavenumber (cm^{-1})	Vibration type
570	S-O
1020	O=S=O

729	Vibrations of phenyl ring
1508	
1602	
550	Vibrations of pyrrole ring
850	
1064	
1120	
1410	
1166	N-Cu
1643	C=N
1542	
3000-3600	C-H str. and absorbed water

Table S1. FT-IR spectra of Cu-Por

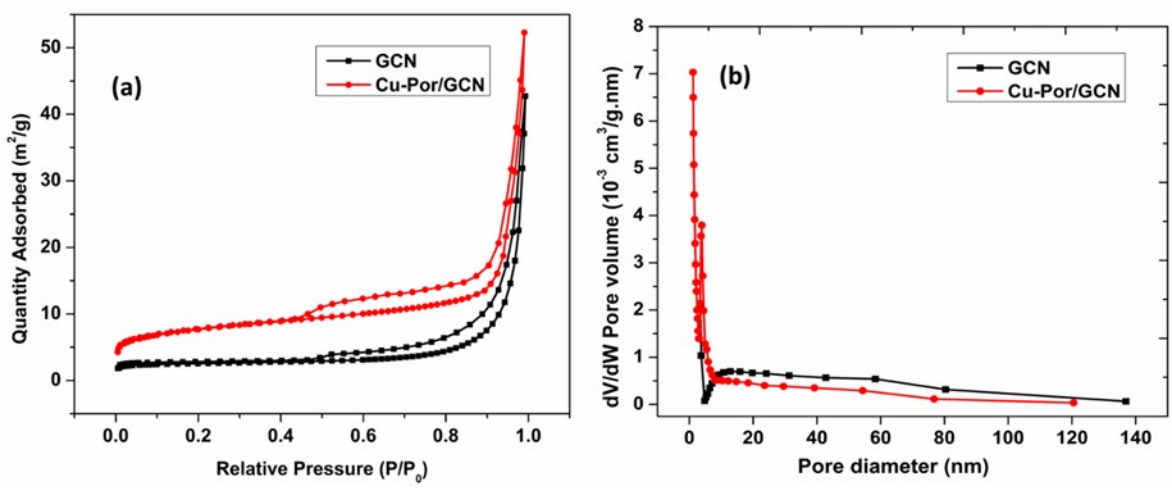

Figure S4. (a)Nitrogen adsorption-desorption isotherms and (b) BJH pore size distribution of GCN and Cu-Por/GCN

Photocatalyst	**Surface area (m^2/g)**	**Mean pore diameter (nm)**	**Pore volume (cm^3/g)**
GCN	8.00	6.12	0.06
Cu-Por/GCN	35.25	23.43	0.17

Table S2. (a)Surface area (B) Mean pore diameter and (c) pore volume of GCN and Cu-Por/GCN

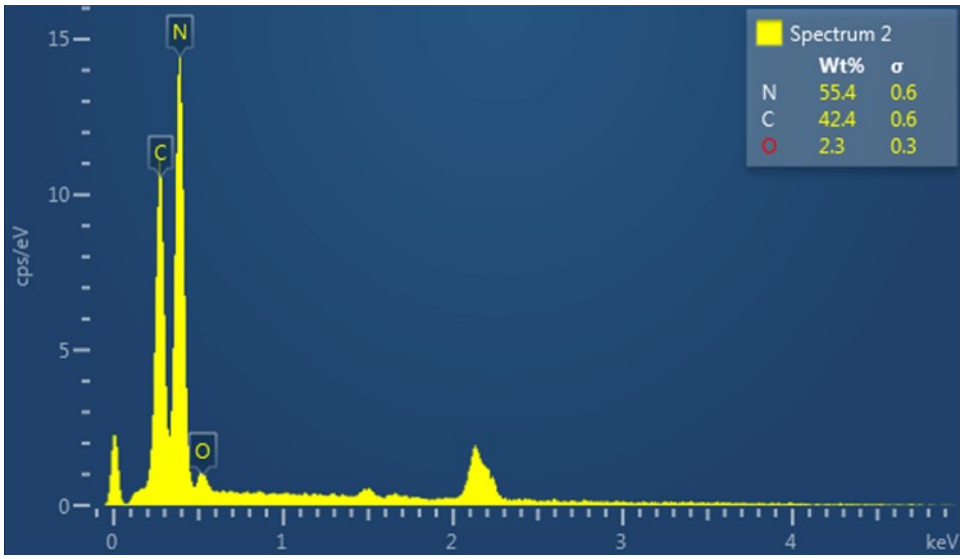

Figure S5. EDS spectrum of GCN.

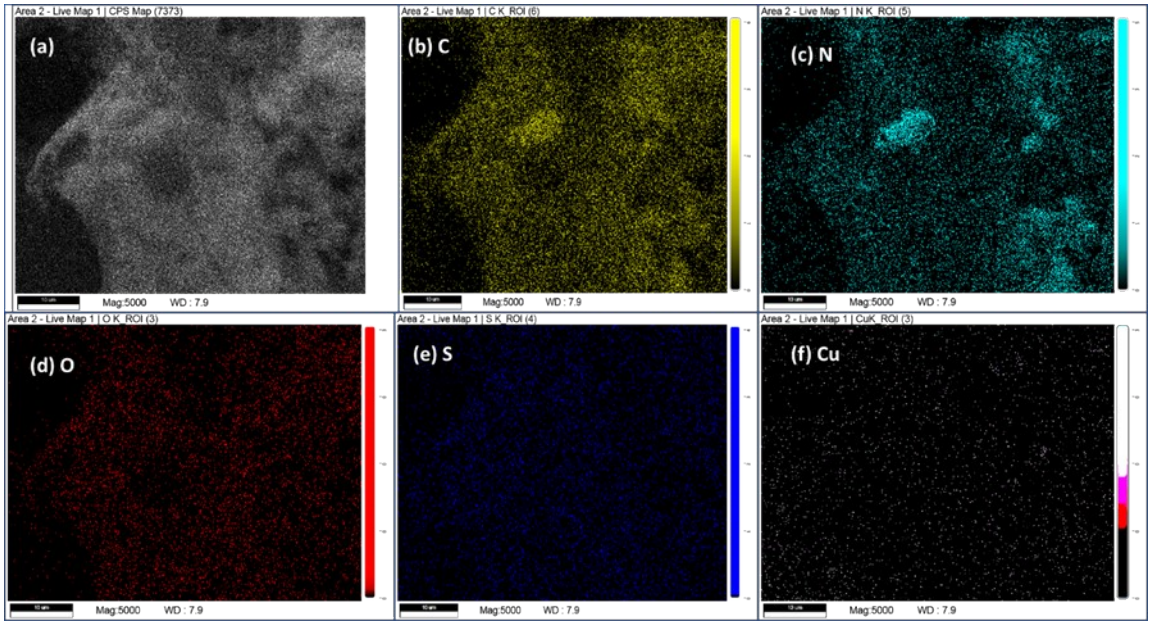

Figure S6. EDS Mapping of Cu-Por/GCN

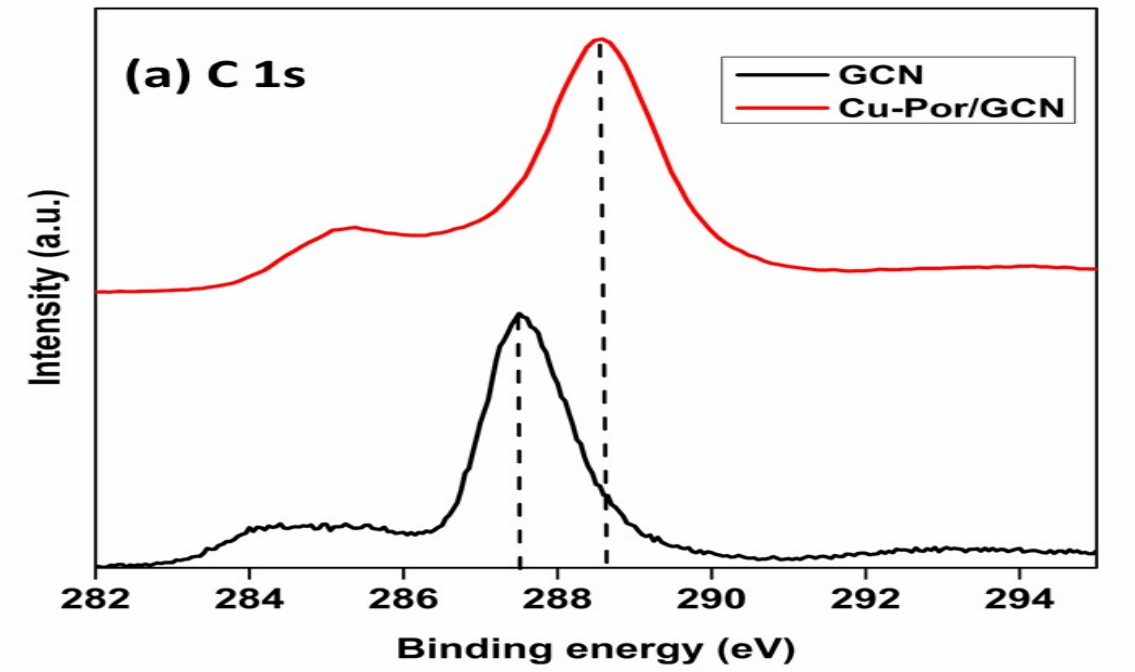
(a) C 1s
GCN
Cu-Por/GCN
Intensity (a.u.)
282
284
286
288
290
292
294
Binding energy (eV)

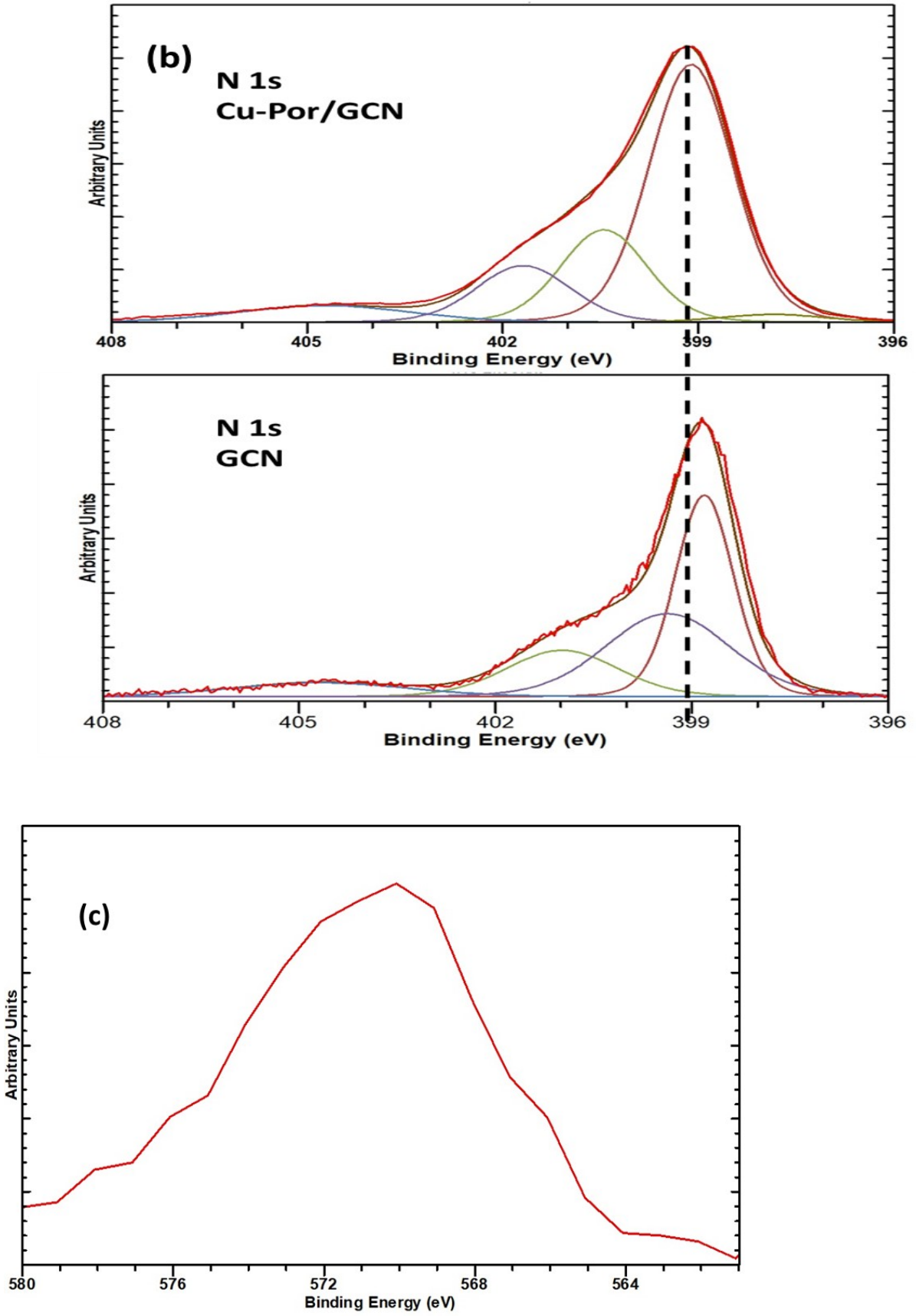

Figure S7. Shift of peak in Cu-Por/GCN in comparison with GCN in (a) C 1s and (b) N 1s (c) Cu LMM peak

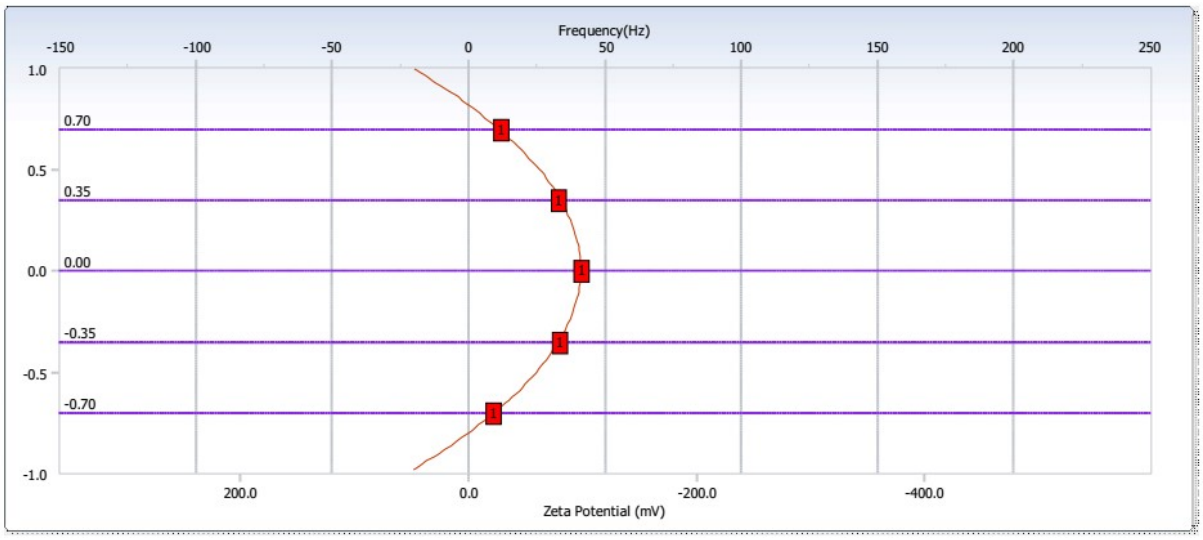

Figure S8. Zeta potential of GCN

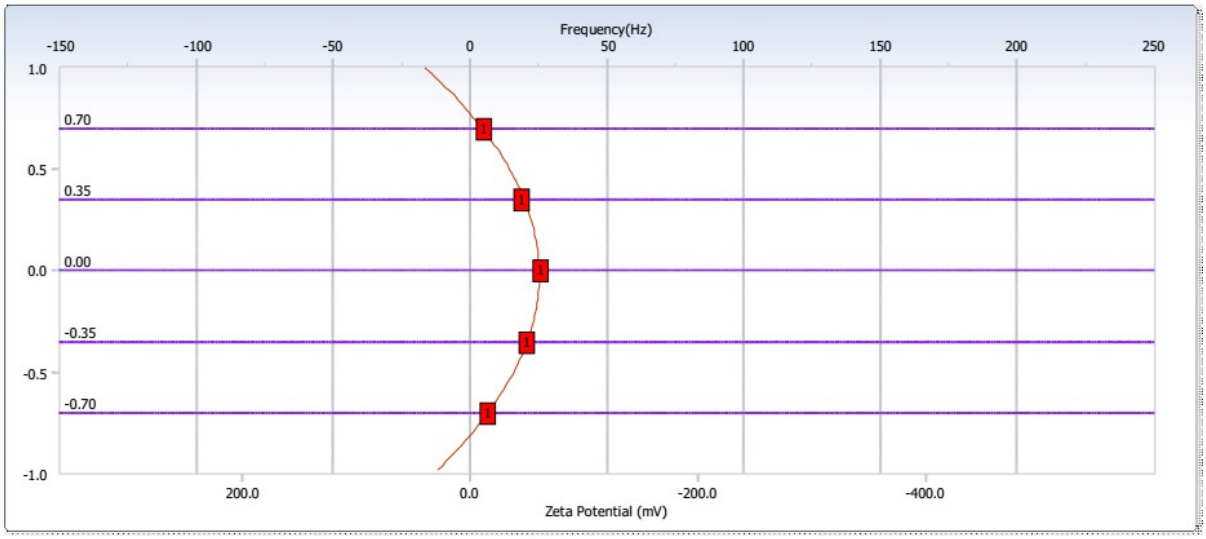

Figure S9. Zeta potential of Cu-Por/GCN

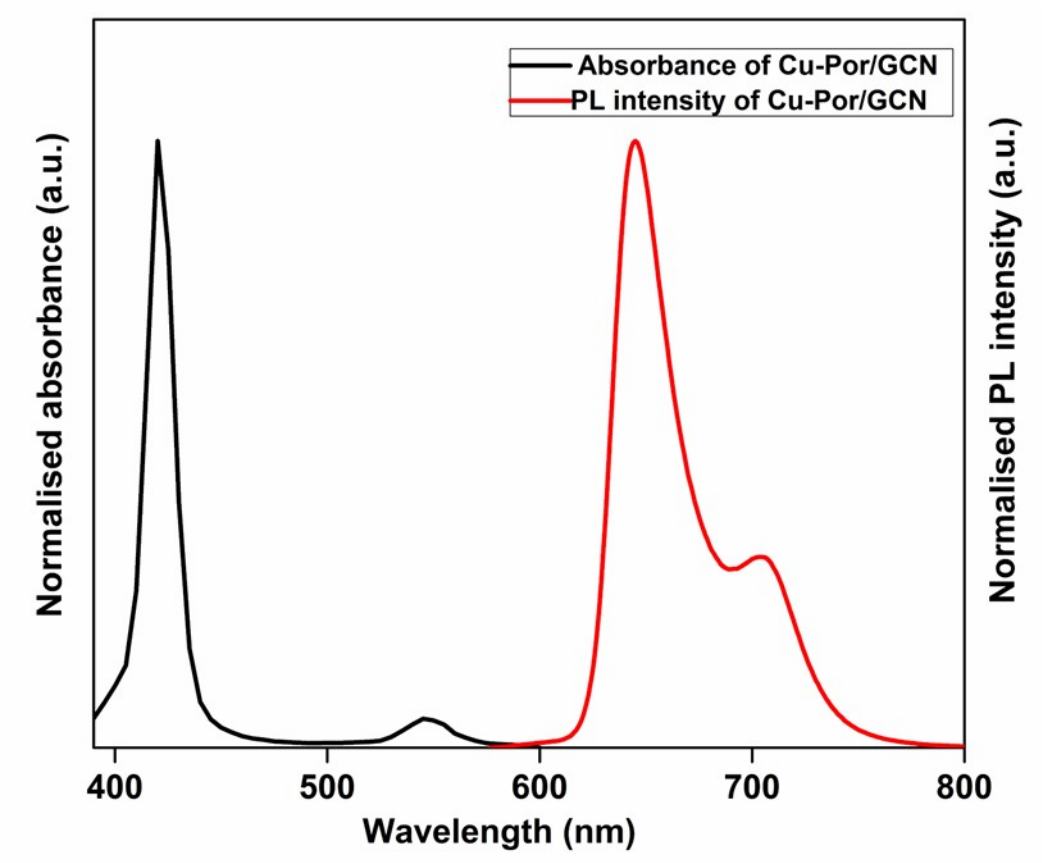

Figure S10. Comparison of absorbance and PL of Cu-Por/GCN

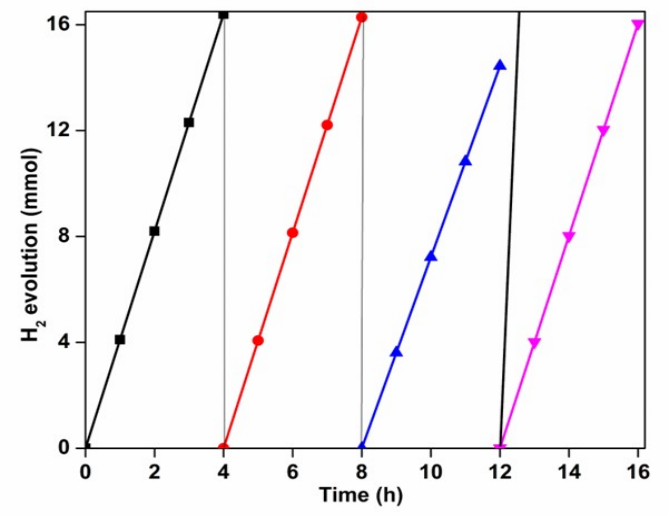

Figure S11. (c) Recyclability of Cu-Por/GCN

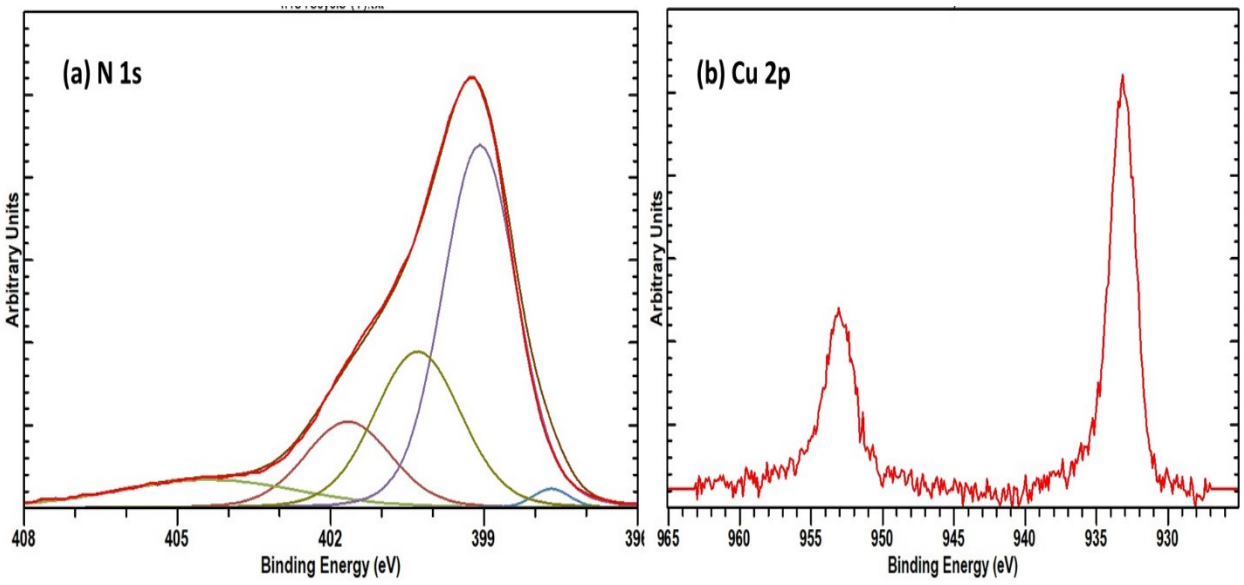

Figure S12. (a) N 1s and (b) Cu 2p XPS spectra of reused Cu-Por/GCN

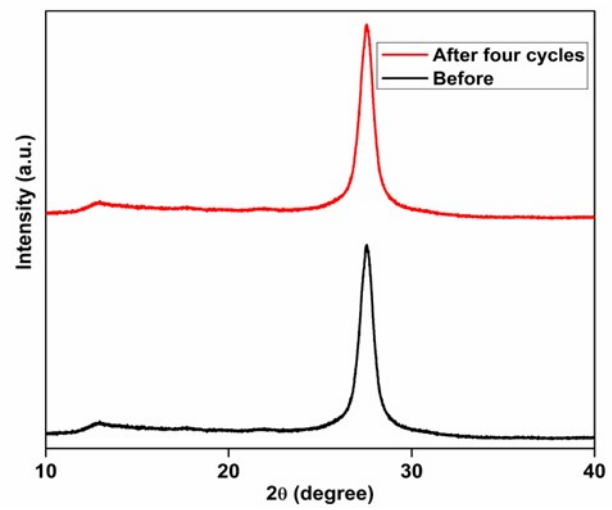

Figure S13. Comparison of XRD of Cu-Por/GCN before and after four cycles.

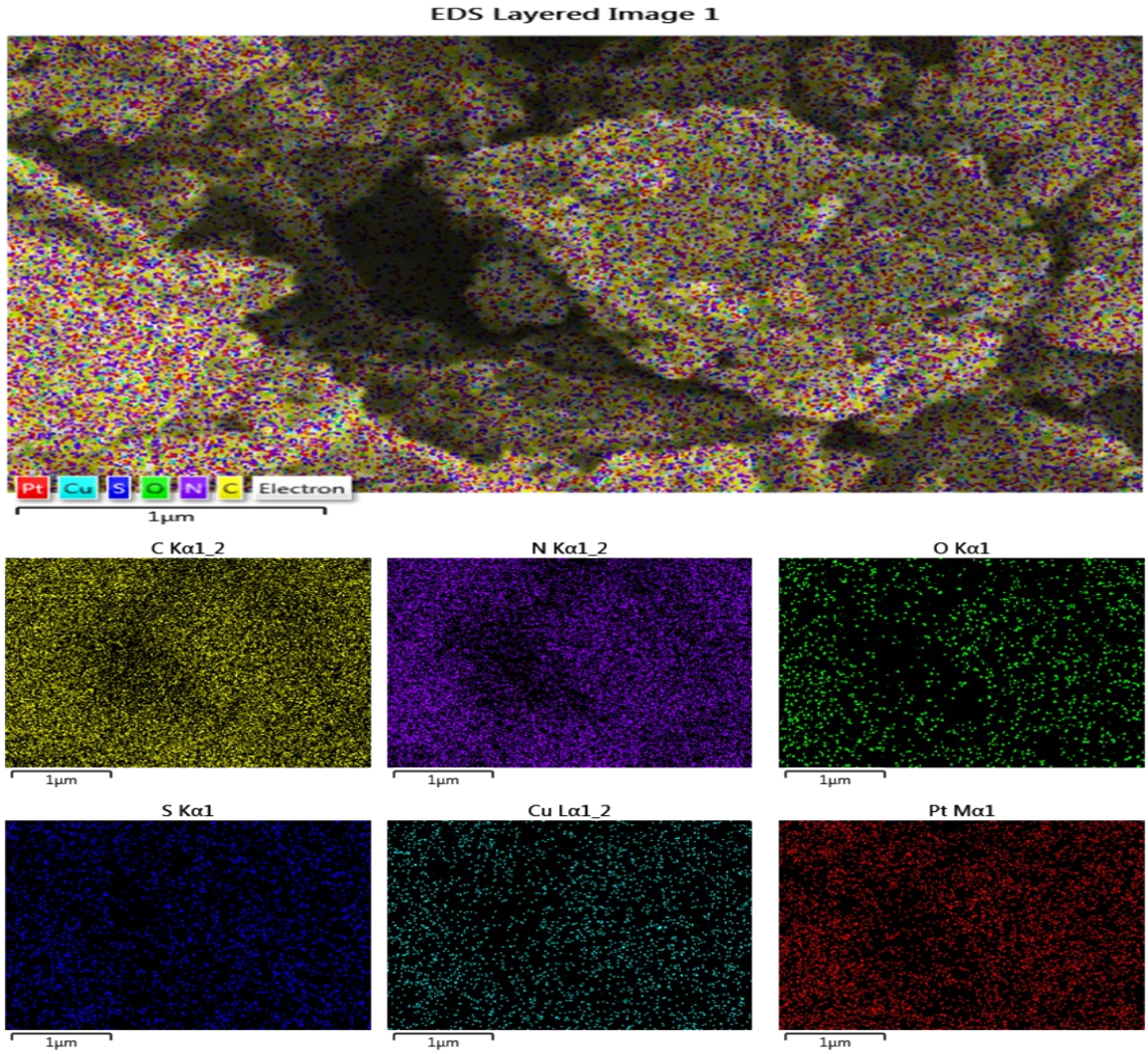

Fig. S14: SEM/EDS and mapping of Cu-Por/GCN after photocatalysis.

Ref. No.	Catalyst	Cu content (%)	H_2 evolution (µmol g^{-1} h^{-1})	AQY (%)
S5.	Cu-Cu_2O/GCN	7	400	NA
S6.	Cu_2O@GCN	83.2	795	NA
S7	Cu_2O-GCN	0.93	842	NA
S8.	Cu_3P/g-C3N	1	343	NA
S9.	$Cu_2(OH)_2CO_3$	3	22.6	NA
S10.	Cu/GCN	45	3774.35	1.34
S11	CuS/GCN	2	348	NA
S12	Cu_3P/GCN	1	284	2.6
S13	CuNiS/GCN	2	758.2	4.38
	Copper tetraphenylporphyrin tetrasulphonic acid/ GCN (This work)	0.6	4100	65.1

Table S3: Comparison of photocatalytic H_2 evolution various copper containing GCN based catalysts.

References

S1. L. Yanfei, M. He, R. Guo, Z. Fang, K. Shifei, Z. Ma, M. Dong, W. Wenlong and C. Lifeng. Appl. Catal., B.,2020, 260, 118137.

S2. K. Zhu, M. Zhang, X. Feng, L. Qin, S. Z. Kang and X. Li, Appl. Catal., B, 2020, 268, 118434.

S3. H. Zhang, R. Zhang, X. Liu, F. Ding, C. Shi, Z. Zhou and N. Zhao, J. Mater. Chem. A, 2021, 9, 24915–24921.

S4. I. Elsayed , M. Mashaly , F. Eltaweel , M. A. Jackson and E. B. Hassan , Fuel, 2018, 221 , 407 —416.

S5. P. Zhang, T. Wang and H. Zeng, Appl. Surf. Sci., 2017, **391**, 404-414.

S6. L. Liu, Y. Qi, J. Hu, Y. Liang and W. Cui, Appl. Surf. Sci., 2015, **351**, 1146-1154.

S7. S. Anandan, J. J. Wu, D. Bahnemann, A. Emelin and M. Ashokkumar, 2017, **527**, 34-41.

S8. H. Zhou, R. Chen, C. Han, P. Wang, Z. Tong, B. Tan, Y. Huang and Z. Liu, J. Colloid Interf. Sci., 2022, 610, 126-135

S9. Y. Liu, X. Wu, H. Lv, Y. Cao and H. Ren, Dalton Trans., 2019, **48**, 1217-1225

S10. C. Wang, J. Xie, Ning Chen, Weifeng Chen, Penghui Bai and Hu Wang, ACS Appl. Energy Mater, 2021, **4**, 13796−13802.

S11. R. Shen, J. Xie, P. Guo, L.0 Chen, X. Chen and X. Li, ACS Appl. Energy Mater., 2018, **1**, 2232-2241.

S12. Z. Qin, M. Wang, R. Li and Y. Chen, Sci. China Mater., 2018, **61**, 861-868

S13. W. Wang, Y. Tao, L. Du, Z. Wei, Z. Yan, W.K. Chan, Z. Lian, R. Zhu, D.L. Phillips and G. Li, Appl. Catal., B, 2021, **282**, 119568